May, 2006

Negative Coulomb Damping, Limit Cycles, and Self-Oscillation of the Vocal Folds

Lewis P. Fulcher, *Bowling Green State University - Main Campus*
Ronald Callaway Scherer, *Bowling Green State University*
Artem Melnykov, *Bowling Green State University - Main Campus*
Vesela Gateva, *Bowling Green State University - Main Campus*
Mark E. Limes, *Bowling Green State University - Main Campus*

Negative Coulomb damping, limit cycles, and self-oscillation of the vocal folds

Lewis P. Fulcher[a)]
Department of Physics and Astronomy, Bowling Green State University, Bowling Green, Ohio 43403

Ronald C. Scherer[b)]
Department of Communication Disorders, Bowling Green State University, Bowling Green, Ohio 43403

Artem Melnykov,[c)] Vesela Gateva, and Mark E. Limes
Departments of Physics and Astronomy, Bowling Green State University, Bowling Green, Ohio 43403

(Received 11 June 2005; accepted 6 January 2006)

An effective one-mass model of phonation is developed. It borrows the salient features of the classic two-mass model of human speech developed by Ishizaka, Matsudaira, and Flanagan. Their model is based on the idea that the oscillating vocal folds maintain their motion by deriving energy from the flow of air through the glottis. We argue that the essence of the action of the aerodynamic forces on the vocal folds is captured by negative Coulomb damping, which acts on the oscillator to energize it. A viscous force is added to include the effects of tissue damping. The solutions to this single oscillator model show that when it is excited by negative Coulomb damping, it will reach a limit cycle. Displacements, phase portraits, and energy histories are presented for two underdamped linear oscillators. A nonlinear force is added so that the variations of the fundamental frequency and the open quotient with lung pressure are comparable to the behavior of the two-mass model.
[DOI: 10.1119/1.2173272]

I. INTRODUCTION

Peters and Pritchett[1] have considered a variety of applications of oscillatory systems subject to dry sliding friction. Their applications include the linear oscillator and the small-amplitude pendulum, which they gave the colorful name, the "flip-flop" pendulum. They presented a theoretical analysis and amplitude measurements to support their observation that a constant frictional force implies that the amplitude decays linearly with time, rather than the exponential decay associated with linear viscous damping. Their analysis was based on an application of Newton's law,

$$m\ddot{x} + kx = F_f \,\mathrm{sgn}(x), \tag{1}$$

where m is the mass of the oscillator, k is the spring constant, and F_f is the constant force associated with kinetic friction, as shown in Fig. 1. The function $\mathrm{sgn}(x)$ denotes the sign of the velocity and ensures that the friction term has the appropriate sign. Barratt and Strobel treated a mass-spring system with dry friction on an inclined plane, with a driving force that allows acceleration up and down the plane with different magnitudes.[2] Squire considered a rigid pendulum with dry friction and linear and quadratic viscous forces.[3] He also discussed experimental procedures for equipping the pendulum such that one of the damping mechanisms would be dominant. By adding a fibrous rubber brake pad to the pendulum, he gave a convincing demonstration of the linear decay law for the pendulum's amplitude, which is characteristic of dry friction. Lapidus[4] emphasized the conditions necessary for a given number of oscillations, and Hudson and Finfgeld[5] used Laplace transform techniques to solve the equation of motion. Oscillatory motion in the presence of dry friction has been studied in detail in some of the classic works of nonlinear dynamics,[6,7] where it is usually called the Coulomb frictional force.

Linear oscillating systems with Coulomb friction are isochronous, that is, the period of the motion does not depend on the magnitude of the frictional force or on the amplitude of the motion, although the amplitude decrease is proportional to the magnitude of the frictional force. (The frictional force must be small enough to permit oscillations.[4]) Thus the angular frequency of the motion described by Eq. (1) is $\omega_0 = (k/m)^{1/2}$. This behavior is in contrast to that of linear viscous damping where the angular frequency depends on the strength of the damping force according to[8,9] $\omega = (k/m - \gamma^2)^{1/2}$, where γ is the damping parameter. The linear oscillator with linear damping also is isochronous in that the angular frequency does not depend on the amplitude.

The Coulomb damping force in Eq. (1) changes sign as the velocity of the oscillator changes sign. Thus the power delivered to the oscillator by the frictional force is negative for both positive and negative velocities, resulting in negative work for each cycle of the motion. This negative work decreases the energy of the oscillator, so that its turning points move closer and closer to the equilibrium position. At some point in the motion the turning point is close enough to the equilibrium position so that the restoring force is unable to overcome the frictional force, and the oscillator comes to rest. These features also emerge from a straightforward work-energy analysis of the linear oscillator with Coulomb friction.[10]

Changing the sign of the force on the right-hand side of Eq. (1) would result in positive work being done by the driving force. Such a force, which we call negative Coulomb damping, would add energy to the oscillator during each cycle. The amplitude of the oscillator will grow linearly and become unbounded. For this reason we add a viscous damping force to Eq. (1) so that there is a mechanism to add energy (negative Coulomb damping) and a mechanism to remove energy (viscous damping) during the motion. If an oscillator at rest is subject to both of these forces, we would expect increases of the amplitude and the speed until the viscous damping losses become equal to the energy gains.

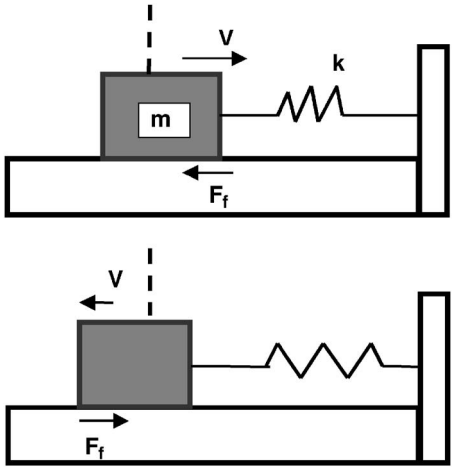

Fig. 1. Harmonic oscillator with dry sliding friction. The dashed vertical line represents the location of the equilibrium position of the oscillator.

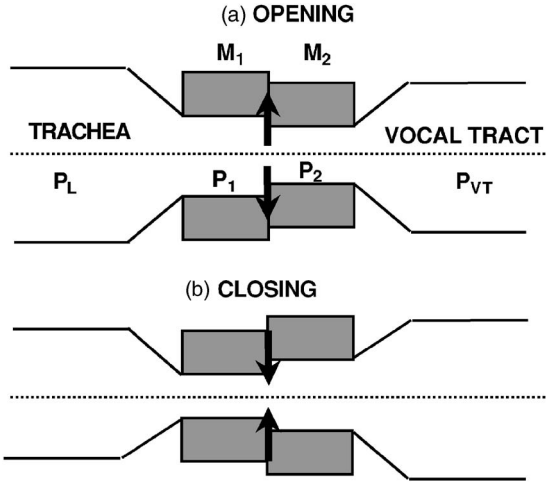

Fig. 2. Schematic representation of the two-mass model of Ishizaka, Matsudaira, and Flanagan (Ref. 12) and its configurations during the opening and closing motions.

Thus we would expect stable oscillatory behavior similar to the limit cycles of a van der Pol oscillator or a Rayleigh oscillator.[11] In the following we show that a limit cycle emerges from this combination of negative Coulomb damping and linear viscous resistance in the long-time limit.

II. PHONATION AND THE TWO-MASS MODEL OF ISHIZAKA, MATSUDAIRA, AND FLANAGAN

Human speech involves the use of the larynx to produce voiced sounds such as the English vowels, voiced consonants such as b,d,m,l, and other communicative sounds such as grunts and humming. Voicing occurs when the two vocal folds in the larynx come close to each other and are placed into vibration by forces acting on them from the airflow through the larynx. The tracheal air pressure is close to the value of the lung pressure created by expiratory forces. Each of the vocal folds is made of mucosal and muscle tissue and thus has biomechanical properties. The two-mass model of each of the vocal folds developed by Ishizaka, Matsudaira, and Flanagan[12,13] (IMF) was an important step in understanding human phonation, because it explained how energy can be transferred from the flow of air between the vocal folds to sustained oscillations.[14] Oscillations of the vocal folds with sufficient amplitude, which requires a threshold of pressure, act as a valve to chop the flow of air from the lungs into pulses of short duration. These pulses are introduced into the vocal tract as acoustic excitations and are shaped by the vocal tract resonances into the phonemes familiar in human speech. When the vocal folds are separated, the space between them is called the glottis.

The two-mass model of IMF represents the vocal folds as two sets of opposing masses, with the freedom to oscillate laterally in response to the forces on their medial (toward the center of the glottis) surfaces produced by the flow of air from the lungs (see Fig. 2). Each set of masses executes a motion that is a mirror image of the other set, and thus the two-mass model requires only two degrees of freedom to describe the oscillatory behavior of the vocal folds. In response to the flow of air, the intraglottal pressures P_1 and P_2, the pressures inside the glottis, differ from the lung pressure P_L and the pressure in the vocal tract P_{VT}. The elevated lung pressure produces a flow of air through the glottis in accord with the IMF treatment[12,13] of the Bernoulli effect and of viscosity.

The key to understanding the self-oscillating mechanism of the two-mass model is knowledge of the sequence of shapes that occur during a complete cycle of vocal fold motion. As depicted in Fig. 2(a), the upstream mass M_1, at the leading edge of the vocal folds, is further from the midline than the downstream mass M_2 during the opening phase of the motion, and the glottis has a converging shape when opening. The IMF treatment of airflow gives intraglottal pressures that are higher than the pressure in the vocal tract for converging shapes. Thus, the net force (represented by the large arrows) on the vocal folds is away from the midline and in the same direction as the velocity, and the force due to the airflow does positive work on the vocal folds during the opening phase. As depicted in Fig. 2(b) the leading edge of the vocal folds is closer to the midline than the trailing edge during the closing phase of the motion, which gives a diverging shape for the glottis during the closing phase. The IMF treatment of airflow gives intraglottal pressures that are lower than the pressure in the vocal tract for diverging shapes, and the net force on the vocal folds is toward the midline, which is also in the same direction as the velocity. Thus positive work is also done on the vocal folds by the airflow during the closing phase. Because the air stream on the vocal folds does positive work during both the opening and closing phases, there is a net transfer of energy from the air stream to the vocal folds during each cycle.[15–18]

We see that the effect of the airflow mechanism is similar to the energy transfer process due to negative Coulomb damping. Part of the appeal of the two-mass model is that the sequence of shapes shown in Fig. 2 is a natural consequence of the dynamics of the model, whose equations result in the phase of the second oscillator following that of the first by about 60°.

Because self-oscillation requires different shapes during the opening and closing phases of the motion, we would expect this behavior to depend sensitively on the stiffness of the spring coupling the two masses. The parameter search by Ishizaka and Flanagan[12] shows that the self-oscillation property disappears in the limit of large spring stiffness. Thus, the

two-mass model provides a natural explanation for the difficulty that Flanagan and Landgraf[19] found in their attempt to create a one-mass model of self-oscillation. Their model did not have enough freedom to allow for the required converging and diverging shapes of the two-mass model, and hence their model could not achieve self-oscillation unless a vocal tract was added. Under the right circumstances, the vocal tract enhances the effects of the lateral driving forces to the point where self-oscillation is possible.

III. AN EFFECTIVE ONE-MASS MODEL

In spite of the difficulties encountered in Ref. 19, it should be possible to create a one-mass model of the self-oscillating vocal folds because a transformation from the coordinates of the two oscillators of Fig. 2 to a set consisting of the center of mass of the two oscillators and their relative coordinate should not alter the physics. If we argue that the energy of the relative coordinate does not play an essential role and that the relative coordinate merely acts as a switch to change the shape of the glottal channel at the appropriate times, then the stage is set for a mechanism that gives self-oscillation. In particular, the switch changes the glottal shape so that the lateral aerodynamic forces acting on the vocal folds are always in phase with the velocity of the vocal folds and hence do positive work on them, as indicated by the arrows of Fig. 2. The equation of motion for such a driven oscillator is

$$m\ddot{x} + r\dot{x} + kx = F_0 \quad (x \geqslant 0), \tag{2}$$

and

$$m\ddot{x} + r\dot{x} + kx = -F_0/2 \quad (x < 0), \tag{3}$$

where r measures the strength of the viscous damping. In our model the force F_0 is taken to be the lung pressure P_L multiplied by the area of the medial surface of the glottis (1.2 cm by 0.3 cm). The pressure in the vocal tract is taken to be atmospheric pressure.

From the right-hand sides of Eqs. (2) and (3) we see that allowance has been made for a weaker driving force when the oscillator moves toward the midline than when the oscillator moves away from the midline. This dichotomy is a consequence of a difference in the behavior of the pressure distributions of the two-mass model for converging and diverging shapes, as explained in connection with Fig. 2. We may obtain the ratio of these two forces from the two-mass model by calculating the intraglottal pressures along the medial surfaces of the two masses of Fig. 2 for the appropriate converging and diverging shapes. An alternative is to examine the pressure distributions of a scaled plastic model of the larynx[16,17] for the appropriate converging and diverging shapes. Both approaches yield a relation for the ratio of these two driving forces that is a complicated function of the pressure and the oscillator coordinates. In general, the driving force for the inward motion is weaker than for the outward motion, and a factor of 2 is a reasonable choice to include the effects of this difference.

If the oscillator is assumed to be at rest at the origin when the lung pressure is elevated at $t=0$, the solution of Eq. (2) is given by

$$x(t) = \bar{x}[1 - \sec\phi e^{-\gamma t}\cos(\omega t + \phi)], \tag{4}$$

where $\gamma = r/(2m)$, $\omega = (k/m - \gamma^2)^{1/2}$, and $\bar{x} = F_0/k$ is the characteristic displacement associated with the driving force. The phase ϕ is determined from the relation $\tan\phi = -\gamma/\omega$. Equation (4) describes the motion until the oscillator reaches the first turning point at time t_1 where $\dot{x}(t_1) = 0$. This point occurs at $t_1 = \pi/\omega$, and hence the first turning point is given by

$$x_1 = x(t_1) = \bar{x}[1 + e^{-\gamma\pi/\omega}]. \tag{5}$$

To find the second turning point, we need to solve Eq. (3) subject to the initial conditions $\dot{x}(t_1) = 0$ and Eq. (5) for $x(t_1)$. This solution to Eq. (3) takes the form

$$x(t) = -\bar{x}[3e^{\gamma\pi/\omega}/2 + 1]\sec\phi e^{-\gamma t}\cos(\omega t + \varphi) - \bar{x}/2, \tag{6}$$

where $\tan\phi = -\gamma/\omega$ as in Eq. (4). [In the following equations the phase ϕ is the same as that in Eq. (4).] The analytic form of Eq. (6) allows us to find the second turning point at time t_2, which is defined by the condition $\dot{x}(t_2) = 0$. This point occurs at $t_2 = 2\pi/\omega$, and thus

$$x_2 = x(t_2) = -\bar{x}[3e^{-\gamma\pi/\omega}/2 + e^{-2\gamma\pi/\omega} + 1/2]. \tag{7}$$

As time progresses beyond t_2, the equation of motion again becomes Eq. (2). This equation is subject to the initial conditions $\dot{x}(t_2) = 0$ and Eq. (7) for $x(t_2)$. Its solution is

$$x(t) = -\bar{x}[3e^{\gamma\pi/\omega}/2 + 3e^{2\gamma\pi/\omega}/2 + 1]\sec\phi e^{-\gamma t} \times\cos(\omega t + \phi) + \bar{x}. \tag{8}$$

As before, we can find the time $t_3 = 3\pi/\omega$ at which the third turning point occurs. The expression for x_3 is

$$x_3 = x(t_3) = \bar{x}[3e^{-\gamma\pi/\omega}/2 + 3e^{-2\gamma\pi/\omega}/2 + e^{-3\gamma\pi/\omega} + 1]. \tag{9}$$

From Eqs. (5) and (9) one may infer that all odd-numbered turning points are maxima and all even-numbered turning points are minima. The nth oscillation begins at time t_{2n-1} and ends at time t_{2n+1}.

The condition $\dot{x}(t_n) = 0$ requires that $t_n = n\pi/\omega$. The relation between the height of the maximum at t_n and the minimum at t_{n+1} is given by

$$x_{n+1} + \bar{x}/2 + (x_n + \bar{x}/2)e^{-\gamma\pi/\omega} = 0 \quad (n \text{ odd}). \tag{10}$$

By considering the second half of this oscillation, we obtain a relation between the minimum x_{n+1} and the next maximum

$$x_{n+2} - \bar{x} + (x_{n+1} - \bar{x})e^{-\gamma\pi/\omega} = 0. \tag{11}$$

Equations (10) and (11) may be used to relate the amplitudes of two successive maxima,

$$x_{n+2} = x_n e^{-2\gamma\pi/\omega} + \bar{x}[1 + 3e^{-\gamma\pi/\omega}/2 + e^{-2\gamma\pi/\omega}/2]. \tag{12}$$

We can solve the recurrence relation in Eq. (12) to find an explicit expression for the maximum at t_n, namely,

$$x_n = \bar{x}[1 + 3(e^{-\gamma\pi/\omega} + e^{-2\gamma\pi/\omega} + \cdots + e^{-(n-1)\gamma\pi/\omega})/2 + e^{-n\gamma\pi/\omega}]. \tag{13}$$

The geometric series in the parentheses of Eq. (13) may be summed. For large n the last term becomes unimportant, and Eq. (13) approaches the limit,

$$x_n \to \bar{x}[1 + 3(e^{\gamma\pi/\omega} - 1)^{-1}/2] \quad (n \text{ odd}). \tag{14}$$

A similar procedure yields the following result for the minimum at t_{n+1}:

$$x_{n+1} \to -\bar{x}[1/2 + 3(e^{\gamma\pi/\omega} - 1)^{-1}/2]. \tag{15}$$

From Eqs. (14) and (15) a center of oscillation $x_c = (x_n + x_{n+1})/2 = \bar{x}/4$ may be defined and the large-n difference of the maxima and minima may be determined,

$$x_{n+2} - x_{n+1} = 3\bar{x}\, ctnh(\gamma\pi/2\omega)/2. \tag{16}$$

If we subtract the value of the center of oscillation from the expressions for x_n and x_{n+1} in Eqs. (14) and (15), we see that the oscillation is symmetric about this center in the limit of large n.

Inspection of Eqs. (14)–(16) reveals that none of these limits depends on n, and thus in the large n limit, all reference to the history of the motion disappears.[20] This behavior is consistent with the requirements of a limit cycle.[11,21]

IV. LIMIT OF NO VISCOUS DAMPING

The limit $\gamma \to 0$ in Eq. (12) leads to the simplified expression,

$$x_{n+2} = x_n + 3\bar{x}. \tag{17}$$

If Eq. (17) is combined with the $\gamma \to 0$ limit of Eq. (5), we obtain the sequence

$$x_{\max} = [2\bar{x}, 5\bar{x}, 8\bar{x}, 11\bar{x}, \cdots], \tag{18}$$

for the maxima at the first, third, fifth, etc., turning points. An analogous sequence may be found for the minima at the second, fourth, sixth, etc., turning points, that is

$$x_{\min} = [-3\bar{x}, -6\bar{x}, -9\bar{x}, -12\bar{x}, \cdots]. \tag{19}$$

These sequences show that the maxima and the minima exhibit linear laws of growth as we would expect.[1–5] We can obtain Eqs. (18) and (19) from Eq. (20) of Ref. 2 by making the substitution $\alpha_- = F_0/m$ for the acceleration down the incline and $\alpha = F_0/(2m)$ for the magnitude of the acceleration up the incline.

V. NUMERICAL SOLUTION

Although the analytic solutions of Sec. III are straightforward, it is simpler to solve the equations of motion numerically, especially if we use the Euler half-step method.[22] We have verified that the implementation of the half-step method with a spreadsheet gives stable, oscillatory solutions to Eqs. (2) and (3). Reference 12 is used as a guide for parameters suitable for the human vocal folds. Hence we choose $m = 0.125$ g, $k = 80\,000$ dynes/cm, and a pressure difference between the lungs P_L and the vocal tract P_{VT} of 7840 dynes/cm^2 (the pressure required to support a column of water 8 cm high). The time step $\Delta = 0.0001$ s is sufficient, although $\Delta = 0.000\,02$ s is required to achieve an accuracy of three significant figures.

In Fig. 3 we show the displacements of the one-mass model with $r = 20$ g/s and $r = 60$ g/s. For comparison, the driving force ($F_0 = 2822$ dynes) divided by k is also shown. For $v > 0$ this ratio gives the fundamental length $\bar{x}$, and for $v < 0$ this ratio gives $-\bar{x}/2$. Figure 3 makes it clear that the driving force is in phase with the oscillator motion and delivers energy to the oscillator, resulting in an energy gain until the limit cycle is reached. From Fig. 3(a) it is apparent that the onset time, that is, the time required for the oscillation to reach its limit cycle, is about 50 ms or longer for the smaller damping parameter. The more strongly damped case of Fig. 3(b) achieves its limit cycle in 15 to 20 ms, in reasonable agreement with Fig. 7 of Ref. 12. The horizontal line near $x = -0.009$ cm in Fig. 3(b) represents the position of the midline of Fig. 2 relative to the equilibrium value of the oscillator. The oscillator must move past the midline to shut off the flow of air from the lungs. According to Ref. 12, 1960 dynes/cm^2 (2 cm of water) is a reasonable value for the phonation threshold pressure, and Eq. (15) yields $x_{\min} = -0.0089$ cm for this pressure. From the location of this line, we can infer that the oscillator spends 4.9 ms of its 8.2 ms period open and 3.3 ms closed, which gives an open quotient of 0.60.

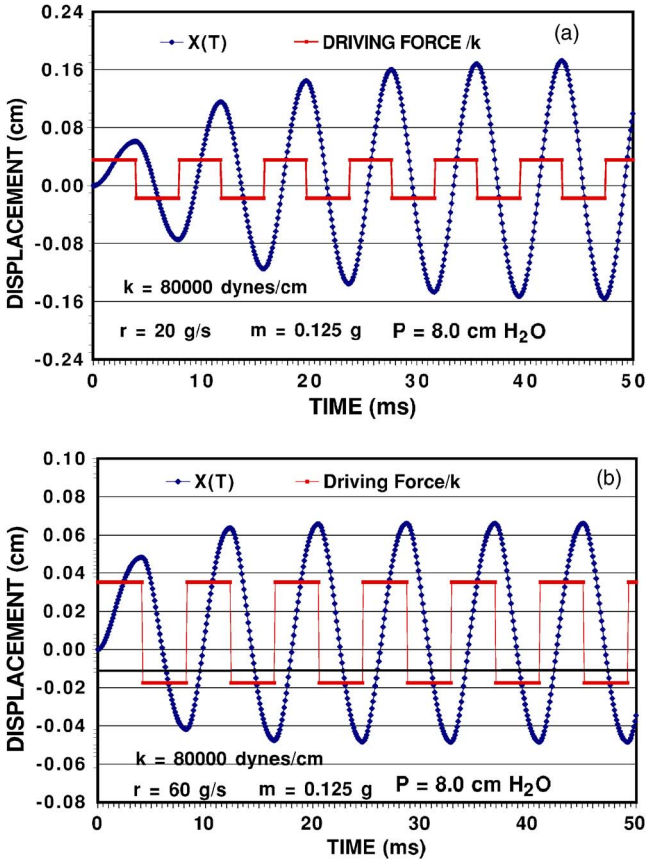

Fig. 3. Displacements of the effective one-mass model for two damping constants. The saw-tooth pattern provides a measure of the driving force.

The phase portraits of Fig. 4 show that both systems approach a limit cycle with well-defined trajectories in phase space, consistent with our expectations from Eqs. (14) and (15). These trajectories, with their outward spirals, suggest a self-limiting behavior characteristic of a limit cycle. To show that this behavior is that of a limit cycle, we must establish that any phase trajectory that begins inside the closed curve of the limit cycle spirals outward to the limit cycle and that any phase trajectory that begins outside the closed curve of the limit cycle spirals inward to the limit cycle. Our numerical simulations with different initial conditions have shown this behavior to be the case, and we conclude that the stable pattern of oscillation exhibited in Figs. 3 and 4 is a limit cycle.

It is apparent that the oscillations in Figs. 3 and 4 have an asymmetry that favors positive displacements, which yields a center of oscillation to the right of the origin, in accord with

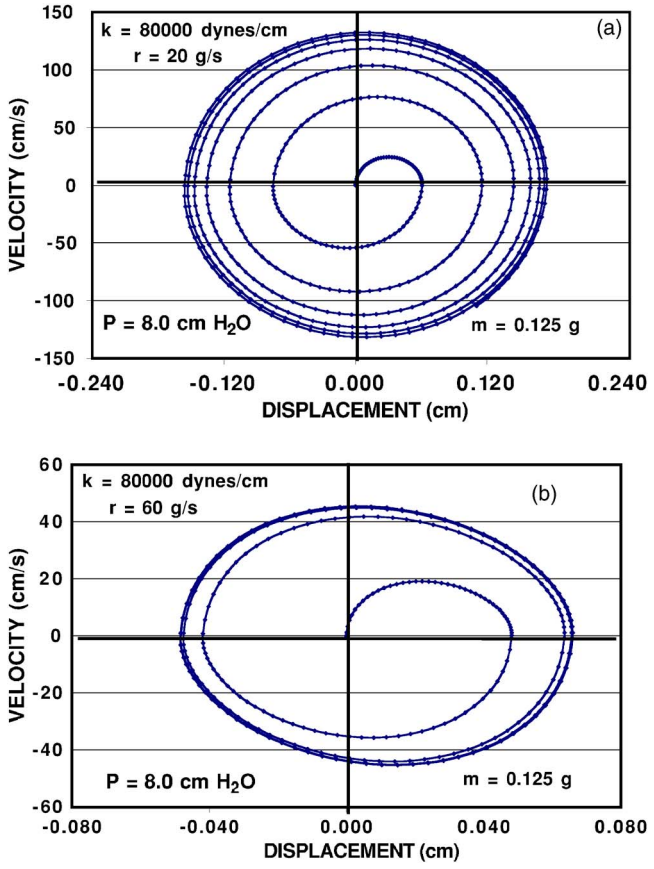

Fig. 4. Phase portraits of the effective one-mass model.

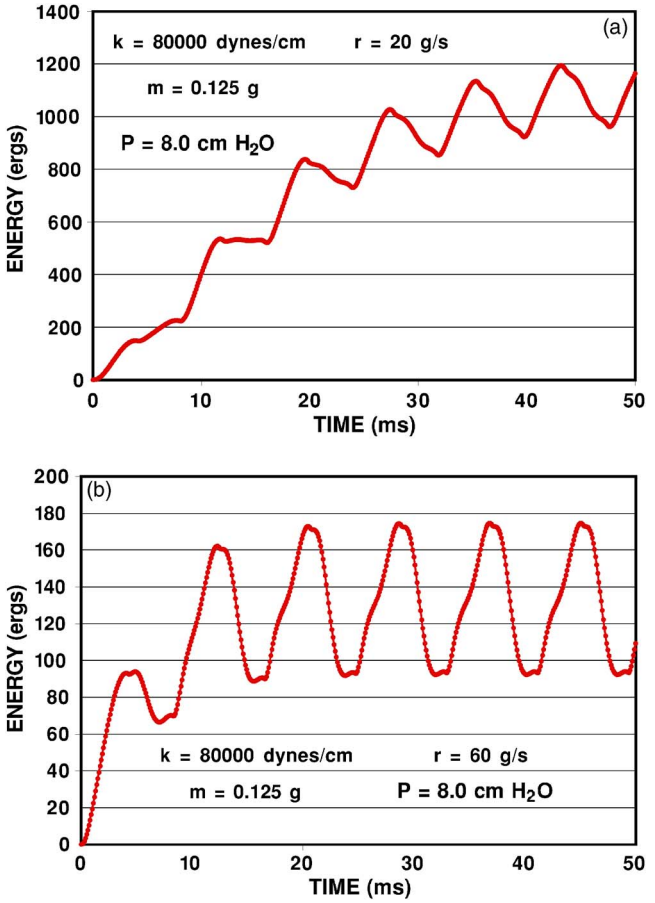

Fig. 5. Time dependence of the total mechanical energy of the oscillating mass in the effective one-mass model.

the result for x_c following Eqs. (14) and (15). Figure 4(b) shows that the limit cycle emerges after about two complete oscillations for r=60 g/s. The rapid development of the limit cycle for the more heavily damped oscillator is also manifest in Fig. 5, where the time dependence of the sum of the kinetic and potential energies for each oscillator is depicted. Note that the same driving force builds up a much larger average energy for lighter damping than for heavier damping, consistent with the requirement of a longer onset time. Thus the ratio of the amplitude of oscillation to the average energy in Fig. 5(a) is much smaller than in Fig. 5(b).

VI. WORK-ENERGY CONSIDERATIONS

If we multiply Eq. (3) by $\dot{x}$ and integrate the resultant equation over a half-cycle of the motion during the closing phase (t_n to t_{n+1}), we find

$$E(t_{n+1}) - E(t_n) = (x_n - x_{n+1})F_0/2 - r\int_{t_n}^{t_{n+1}} \dot{x}^2\, dt \quad (n \text{ odd}) \tag{20}$$

where $E(t)=m\dot{x}^2/2+kx^2/2$ is the total mechanical energy of the oscillator. We multiply Eq. (2) by $\dot{x}$ and integrate the result over the half-cycle of the motion (t_{n+1} to t_{n+2}) and obtain

$$E(t_{n+2}) - E(t_{n+1}) = (x_{n+2} - x_{n+1})F_0 - r\int_{t_{n+1}}^{t_{n+2}} \dot{x}^2\, dt. \tag{21}$$

Adding Eqs. (20) and (21) and taking the limit of long times [where $E(t_{n+2})=E(t_n)$ and $x_{n+2}=x_n$] gives the result

$$3F_0(x_{n+2} - x_{n+1})/2 - r\int_{t_n}^{t_{n+2}} \dot{x}^2\, dt = 0, \tag{22}$$

which embodies the balance between the work done by the aerodynamic forces and the energy dissipated by the viscous forces, after the limit cycle has been reached. The substitution of Eq. (16) into Eq. (22) gives an explicit expression for the energy lost during a complete oscillation,

$$E_{\text{lost}} = r\int_{\text{cycle}} \dot{x}^2\, dt = 9F_0^2\,[ctnh(\gamma\pi/2\omega)]/(4k). \tag{23}$$

The behavior required for the applicability of Eqs. (22) and (23) is apparent from Figs. 3(b) and 5(b), after the limit cycle is achieved, because the maxima of the oscillations there have the same amplitude, as do the minima of the oscillations. For the parameters of Fig. 5(b) we obtain E_{lost} =490 ergs, which is 2.75 times larger than the maximum of the total mechanical energy, $E_{\max}$=178 ergs,[23] showing that the oscillator with r=60 g/s is heavily damped, but not damped enough to be critically damped (for which r =200 g/s). Dividing E_{lost} by the period of the motion gives

an average power loss of 5.95 mW, after the oscillator has achieved its limit cycle.

It is instructive to compare these numbers with the other average powers in the problem. To calculate the energy input from the lungs, we require the average volume velocity U_{gavg} of flow through the glottis. This velocity may be estimated from the Bernoulli relation for the pressure drop within the glottis, that is

$$\Delta P = \rho U_{\text{gavg}}^2/(2.0A_{\text{gavg}}^2), \tag{24}$$

where ρ is the density of air, and A_{gavg} is the glottal area averaged over a complete cycle of vocal fold motion. The quantity A_{gavg} is the product of the glottal length (1.2 cm) and the averaged glottal diameter d_{avg}, which may be taken from Fig. 3(b). Choosing $d_{\text{avg}}=0.068$ cm yields $A_{\text{gavg}}=0.082$ cm^2 and $U_{\text{gavg}}=296$ cm^3/s. Multiplying U_{gavg} by the pressure in the vocal tract (7840 dynes/cm^2) gives an average power input to the larynx of 232 mW, a level far above that required to drive the vocal folds at their limit cycle amplitudes.

It is also instructive to estimate how much of this input power finds its way into acoustical energy. The data collected in Ref. 24 on the vocal intensity characteristics of elderly and normal speakers furnishes a convenient means of doing so. The sound pressure levels for both groups at a distance of 15 cm from the mouth was measured and the lung pressures and the peak values of the airflow rate were also recorded. For one of their groups at the maximum level of effort, the sound pressure level was about 85 decibels for a recorded lung pressure of 7.96 cm H_2O, a value close to that used to calculate the results of Figs. 3–5. Assuming that this sound pressure level is more or less uniform over a hemisphere centered on the mouth, the average acoustical energy output is 0.045 mW, less than 1% of the value required to drive the vocal folds. Our model does not predict other important energies in the phonation process, such as energy losses in the vocal tract and the kinetic energy associated with the airflow out of the mouth.

VII. NONLINEAR FORCES

As we have discussed, an important property of the oscillator described by Eqs. (2) and (3) is its isochronous property, that is, the frequency of the oscillator does not depend on the strength of the driving force, although the amplitude of the oscillation does. One of the important accomplishments of the two-mass model[12,13] was an explanation of the dependence of the fundamental frequency of oscillation on the driving force of the lung pressure. Because the frequency of the linear oscillator depends only on the mass, the spring constant, and the damping constant, the linear oscillator does not allow any variation of the frequency with the strength of the driving force, which is directly proportional to the lung pressure. To incorporate a variation of fundamental frequency with lung pressure into their model, Ishizaka and Flanagan introduced a nonlinear spring force. In effect, their spring constant k became dependent on position

$$k(x) = k(1 + \eta x^2), \tag{25}$$

where $\eta=100$ cm^{-2}.[12] Our calculation of the effect of the lung pressure on the fundamental frequency, determined by substituting Eq. (25) for the factor k in Eqs. (2) and (3), is depicted in Fig. 6, where the behavior of the nonlinear calculation is compared with the isochronous property of the linear oscillator of Secs. III and V. The results from Fig. 11 of Ref. 12 are also presented in Fig. 6 to provide a comparison with the effective one-mass model. Error bars of 2% are added to our results to allow for possible numerical errors.[23]

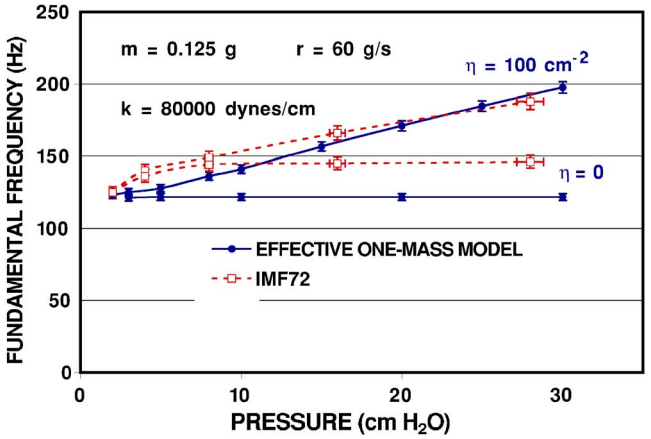

Fig. 6. Pressure dependence of the fundamental frequency for the nonlinear and linear effective one-mass models. The dashed curves are taken from Ref. 12.

Unlike our calculation, the two-mass calculation of Ishizaka and Flanagan[12] used the flow pulses generated by the valve action of the two-mass model as input for a model vocal tract, taken to be a series of four cylinders of total length 16 cm and different cross sections. Their vocal tract was assigned shapes characteristic of different English vowels, such as e and i. For each vowel the environment that the glottal flow pulses encounter on their way to becoming the phonemes of spoken English is different, because each characteristic shape has a distinct set of resonances. The interaction of these resonances with the input flow pulse molds this excitation into the correct form to produce the intended sound. Among other effects, the initial flow pulse experiences a modification of its fundamental frequency, whose magnitude depends on the shape of the vocal tract. For example, near 10 cm H_2O, Ishizaka and Flanagan find the fundamental frequency to be 1% or 2% higher for e than for i. Our results reproduce the linear trend of the two-mass model at higher pressures with a slight difference in the slope. The main differences between our results and the two-mass results are found at lower pressures, where the effects of the interaction with the vocal tract are the largest. The error bars attached to the IMF results of Fig. 6 reflect the frequency spreads associated with the shape of the vocal tract and the difficulties of reading accurately the numbers from Fig. 11 of Ref. 12.

The IMF result for $\eta=0$ in Fig. 6 exhibits the same kind of pressure dependence as their nonlinear result at lower pressures. The influence of the vocal tract on the IMF result for $\eta=0$ almost disappears at higher pressures, resulting in a linear behavior that is nearly parallel to the constant behavior of our $\eta=0$ result.

Our results for the open quotient of the nonlinear one-mass model are presented in Fig. 7 and compared with those of the two-mass calculation. The threshold for both calculations is $P=2.0$ cm H_2O, near the minimum subglotal pressure necessary for vowel production. Both curves exhibit monotonic decreases to values just under 0.6, indicating that

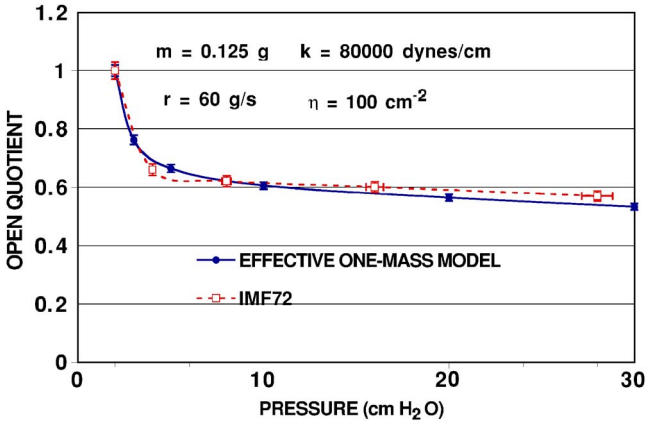

Fig. 7. Pressure dependence of the open quotient of the nonlinear effective one-mass model.

the vocal folds are closed about 40% of the time during the cycle when the driving pressures are large. The open quotient is one of the physiological parameters often monitored in a detailed examination of vocal intensity characteristics.[24] It plays an important role in determining the sharpness of the flow peak, a factor that controls the intensity of the sound radiated.

VIII. SUMMARY

Most treatments of the damped harmonic oscillator focus on viscous damping because of its simplicity, although a constant frictional force also allows an analytical treatment. If the sign of the constant frictional force is changed so that the Coulomb damping force becomes a negative Coulomb damping force, then it can add energy to the oscillator instead of removing it. Adding a viscous damping term makes steady state motion possible. We show that in the long-time limit the analytic solutions approach a limit cycle, and the amplitude and velocity lose their dependence on the history of the motion.

The connection of negative Coulomb damping and viscous friction with the aerodynamic forces on the vocal folds during phonation developed in Refs. 12 and 13 was explored. We explained how an elevated lung pressure gives rise to a flow of air through the glottis and produces a series of alternating converging and diverging shapes of the vertical dimensions of the vocal folds. The pressure distributions in the glottis resulting from this series of shapes are alternately higher and lower than the pressures in the vocal tract. Moreover, these pressure variations are in phase with the motion of the vocal folds, and thus they add energy to the oscillator in the same way as negative Coulomb damping does. The limit cycle of the oscillator with negative Coulomb damping provides a natural explanation of the self-oscillation property of the two-mass model.

Adding a nonlinear driving force to the effective one-mass model eliminates its isochronous property and allows comparison with the results for the pressure dependence of the fundamental frequency and the open quotient obtained with the IMF model. The comparison of Figs. 6 and 7 shows the promise of the effective one-mass model in reproducing more subtle aspects of phonation,[24] in addition to providing a satisfying qualitative explanation of how aerodynamic forces transfer energy to the vocal folds.

ACKNOWLEDGMENTS

The National Institutes of Health Grant No. R01 DC03577 supported this work. The authors would like to thank Guangnian Zhai, Byron Erath, Doug Cook, and Pushkal Thapa for many stimulating conversations and their interest in this project.

[a]Electronic mail: fulcher@bgnet.bgsu.edu
[b]Present address: Department of Otolaryngology, University of Cincinnati Medical Center, Cincinnati, Ohio 45267. Electronic mail: ronald.scherer@uc.edu
[c]Electronic mail: amelnyko@artsci.wustl.edu

[1]Randall D. Peters and Tim Pritchett, "The not-so-simple harmonic oscillator," Am. J. Phys. **65**, 1067–1073 (1997).
[2]C. Barratt and George L. Strobel, "Sliding friction and the harmonic oscillator," Am. J. Phys. **49**, 500–501 (1981).
[3]Patrick T. Squire, "Pendulum damping," Am. J. Phys. **54**, 984–991 (1986).
[4]I. Richard Lapidus, "Motion of a harmonic oscillator with sliding friction," Am. J. Phys. **38**, 1360–1361 (1970).
[5]Robert C. Hudson and C. R. Finfgeld, "Laplace transform solution for the oscillator damped by dry friction," Am. J. Phys. **39**, 568–570 (1971).
[6]N. Minorsky, *Introduction to Non-Linear Mechanics* (Edwards Brothers, Ann Arbor, MI, 1947), pp. 426–433.
[7]Ali H. Nayfeh and Dean T. Mook, *Nonlinear Oscillations* (Wiley, New York, NY, 1979), pp. 125–127.
[8]Lewis P. Fulcher and Brian F. Davis, "Theoretical and experimental study of the motion of the simple pendulum," Am. J. Phys. **44**, 51–55 (1976); Robert A. Nelson and Martin G. Olssen, "The pendulum: Rich physics from a simple system," *ibid.* **54**, 112–121 (1986).
[9]Grant R. Fowles and George L. Cassady, *Analytical Mechanics*, 6th ed. (Saunders, Fort Worth, TX, 1990), pp. 83–92; Vernon D. Barger and Martin G. Olssen, *Classical Mechanics: A Modern Perspective*, 2nd ed. (McGraw-Hill, New York, 1995), pp. 19–25.
[10]Avi Marchewka, David S. Abbott, and Robert J. Beichner, "Oscillator damped by a constant-magnitude frictional force," Am. J. Phys. **72**, 477–483 (2004).
[11]Jerry B. Marion and Stephen T. Thornton, *Classical Dynamics of Particles and Systems*, 4th ed. (Saunders, Fort Worth, TX, 1995), pp. 159–162; N. Minorsky, *Introduction to Non-Linear Mechanics* (Edwards Brothers, Ann Arbor, MI, 1947), pp. 167–182.
[12]K. Ishizaka and James L. Flanagan, "Synthesis of voiced sounds from a two-mass model of the vocal cords," Bell Syst. Tech. J. **51**, 1233–1267 (1972).
[13]K. Ishizaka and M. Matsudaira, *Fluid Mechanical Consideration Of Vocal Cord Vibration*, Monograph No. 8 (Speech Communication Research Laboratory, Santa Barbara, CA, 1972), pp. 1–75.
[14]B. H. Story and Ingo R. Titze, "Voice simulation with a body-cover model of the vocal folds," J. Acoust. Soc. Am. **97**, 1249–1260 (1995).
[15]Our observations of the intraglottal pressures with a scaled plastic model of the glottis support this picture of intraglottal pressures higher than the pressure in the vocal tract for converging shapes and lower than that in the vocal tract for diverging shapes. Our observed intraglottal pressures for the diverging shapes do not lead to fluid forces as large as those predicted by the two-mass model, but they are large enough for the self-oscillation mechanism to operate. Guangnian Zhai (private communication).
[16]R. C. Scherer, D. Shinwari, K. DeWitt, C. Zhang, B. Kucinschi, and A. Afjeh, "Intraglottal pressure profiles for a symmetric and oblique glottis with a divergence angle of 10 degrees," J. Acoust. Soc. Am. **109**, 1616–1630 (2001).
[17]D. Shinwari, R. C. Scherer, K. J. DeWitt, and A. A. Afjeh, "Flow visualization and pressure distributions in a model of the glottis with a symmetric and oblique divergent angle of 10 degrees," J. Acoust. Soc. Am. **113**, 487–497 (2003).
[18]It is not really necessary that the intraglottal pressure be lower than the pressure of the vocal tract during the closing phase for the self-oscillation mechanism to operate. It is only necessary that it be substantially less than the intraglottal pressure during the opening phase, as noted in Ingo R. Titze, "Current topics in voice production mechanisms," Acta Oto-Laryngol. **113**, 421–427 (1993).

[19] James L. Flanagan and Lorinda L. Landegraf, "Self-oscillating source for vocal tract synthesizers," IEEE Trans. Audio Electroacoust. **AU-16**, 57–64 (1968).
[20] The n dependence of the amplitudes in Eqs. (10)–(13) records the history of the motion, because this index indicates which half cycle has been completed. In Fig. 3 of Ref. 1 it is explained how the dependence of the amplitude on n is analogous to a stress-strain hysteresis.
[21] H. Goldstein, C. Poole, and J. Safko, *Classical Mechanics* (Addison-Wesley, San Francisco, 2002), pp. 489–491.
[22] Alan Cromer, "Stable solutions using the Euler approximation," Am. J. Phys. **49**, 455–459 (1981).
[23] The perceptive reader will recognize that the result for the maximum of Fig. 5(b) is nearer 175 ergs, about 2% lower than the value calculated from the analytic expressions. This small (and unimportant) discrepancy is a consequence of a 1% error in the numerical results for the maximum displacement, after the limit cycle has been reached. It may be removed by choosing a smaller step size.
[24] F. Sean Hodge, Raymond H. Colton, and Richard T. Kelley, "Vocal intensity characteristics in normal and elderly speakers," J. Voice **15**, 503–511 (2001).

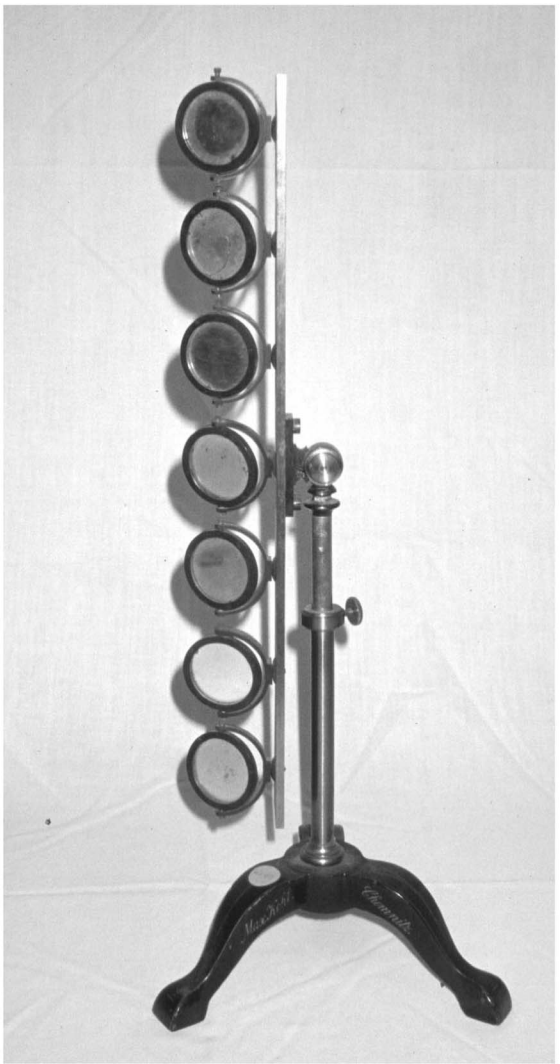

Seven Mirror Device. In Newton's demonstration of the spectrum, a beam of sunlight coming through a small hole in a window blind passes through a triangular glass prism and forms the spectrum on the opposite wall. Newton assumed that there were seven colors: red, orange, yellow, green, blue, indigo and violet. Most of us would omit indigo, but Newton felt that seven was a sacred number. The seven mirror device reverses the process, intercepting seven portions of the spectrum and reflecting them back to a common point on the wall, thus giving white. This example, made by Max Kohl of Chemnitz, Germany and is in the collection of Hobart and William Smith Colleges of Geneva, New York. (Photograph and Notes by Thomas B. Greenslade, Jr., Kenyon College)